ARTICLE

Sustainable Composite of Cardanol Based Phenalkamine Cured Epoxy Systems: Fabrication, Characterization and Mechanical Performance Evaluation for Emerging Applications

Aswinraj Anbazhagan[1], Piyali Roy Choudhury[1], Sahila Sambandam[2] and Jayakumari Lakshmanan Saraswathi[1,*]

[1]Department of Rubber & Plastics Technology, MIT Campus, Anna University, Chennai, 600044, India

[2]Department of Chemistry, Madras Christian College (Autonomous), Affiliated to University of Madras, Tambaram East, Chennai, 600059, India

*Corresponding Author: Jayakumari Lakshmanan Saraswathi. Email: lsjayakumarimit@gmail.com

ABSTRACT

Petroleum-based cured epoxy polymers, used widely in aerospace, marine, and automotive industries, pose environmental threats due to their toxicity. Therefore, developing alternative curing systems for epoxy resin is crucial. This study explores the use of bio-based phenalkamines as curing agents for epoxy resin to enhance the mechanical properties of polymer composites and fiber-reinforced laminates. The functional groups, morphology, and thermal properties of the composites were analyzed using Fourier transform infrared spectroscopy (FTIR), scanning electron microscopy (SEM), and thermogravimetric analysis (TGA). Mechanical properties of two epoxy systems—EP-TETA (triethylenetetramine-cured) and EP-PA (phenalkamine-cured)—were evaluated according to ASTM standards. EP-PA exhibited approximately 318% greater elongation, indicating improved ductility, and 16% higher ultimate force and stress compared to EP-TETA, suggesting its suitability for load-bearing applications. Additionally, phenalkamine-cured epoxy resin composites with adequate thickness demonstrated excellent performance. Glass fiber-reinforced GEP-PA showed 5.3 times greater toughness and adhesion in end notch tests compared to GEP-TETA. These results offer valuable insights for material selection in aerospace and automotive applications.

KEYWORDS

Mechanical properties; phenalkamine; bio-based curatives; fiber reinforced; laminated sheet; triethylenetetramine

1 Introduction

Mechanical properties, in terms of stability and performance, are the key approaches to developing sustainable composite products. In order to make wise decisions in engineering and design, it is essential to comprehend the strength of materials under various loading conditions. Epoxy-based polymers have gathered significant attention due to their versatility and wide-ranging applications

in industries such as aerospace, automotive, construction, and electronics [1–3]. The choice of curing agents plays an important role in the mechanical performance of epoxy-based composites.

In conventional system, formaldehyde and amines as curing agents are involved in condensation reactions to create phenalkamines. Formaldehyde and amines are generally obtained from non-renewable petroleum sources. To reduce the rising expenses and depletion of petrochemical reserves, there is a need to investigate renewable resources as an alternative option. Cardanol is a crucial by-product of the cashew nut industry, obtained from cashew nut shell liquid (CNSL). The CNSL is a naturally occurring mixture of phenolic compounds such as anacardic acid, cardanol, cardol, and 2-methylcardol, with aliphatic side chains [4–6,7]. Hence, CNSL, a sustainable resource, is the source of these agents [8,9]. The CNSL is a main source of naturally occurring phenols obtained from an affordable and easily accessible natural reservoir [10–13]. The agricultural waste generated from cashew nut processing industries is not only used as a coating application but also as brake pad and primer materials for marine applications. Additionally, phenalkamines have a special structure that providestoughnessproperty to the coating applications. However, in our study aims to use phenalkamines as an epoxy-curing agent. This phenalkamines' aromatic backbone provides high chemical resistanceas well as their alkyl side chain adds flexibility, hydrophobicity, and a longer pot life [14].

Phenalkamine curing agents are known for their superior chemical resistance properties for surface coating [15–17]. In recent years, researchers have gained interest in the potential enhancement of the overall performance of epoxy-based materials as cure systems. Additionally, it provides environment-friendly characteristics compared to the existing triethylenetetramine (TETA) cured compound for epoxy. However, there is a lack of research work for optimisation in CNSL-based curing systems for composite materials. The literature currently contains theoretical and experimental results for structural adhesives with intermediate properties. But the conditions and situations were not reported where the adhesive was extremely brittle or highly ductile [18,19]. The current literature, specifically the optimisation of the characterizations and mechanical properties for the automobile and aerospace industries, has not been adequately studied.

It's widely acknowledged that a single-lap joint encounters significant peel loading at the overlap ends, in addition to shear loading. The overall joint strength depends on the adhesive's bonding capacity and its capability to disperse the load across a broader surface, thereby mitigating stress concentration issues [16,17]. Mode I and Mode II fracture toughness tests are generally done to observe the toughness of the reinforced composite laminates. Baere et al. studied and analysed the toughness of carbon fabric-reinforced thermoplastics using Mode I and Mode II fracture toughness tests [20–22]. They have observed unstable crack behaviour in Mode I, while Mode II exhibited stable crack propagation. However, many research articles are available for the TETA-cured system, but there is a lack of articles on PA-cured glass-reinforced laminated sheets. Further scope is there to study the bonding between fiber and matrix in a laminated sheet under a higher loading rate, which could affect the initiation and propagation values [23,24].

In this study, the objective was to use bio-based phenalkamines as curing agents for epoxy resin to enhance the mechanical properties of polymer composite sheets and fiber-reinforced laminates. As per our knowledge, there are no such reports for fiber-reinforced composite laminates with adequate thickness (macro level) made of phenalkamines cured epoxy resin. Moreover, various characterizations, properties, and analyses of performance were conducted. Also, we have compared the mechanical properties of phenalkamine-cured epoxy system (EP-PA) and triethylenetetramine-cured epoxy system (EP-TETA) polymer composite sheets, such as tensile strength, bending behaviour, adhesion strength, and interlaminar fracture toughness. The obtained results can provide insight for material selection in various engineering applications.

2 Experimental

2.1 Materials

Diglycidyl ether of bisphenol A (DGEBA), an Epoxy ResinLY556 and Hardener HY951 were received from Ultimate Enterprises, located in Chennai, India. Phenalkamine, a bio-based curative for epoxy hardening, was received from Satya Cashew Chemicals Pvt. Ltd., Chennai, India. These chemicals were used as such without any further purification.

2.2 Preparation of EP-TETA and EP-PA Samples

Diglycidyl ether of bisphenol A (DGEBA), an epoxy resin is cured with two different curing agents to make polymer composite sheets and is categorised as Sets A and B. In Set A, epoxy is cured with TETA, which is largely available in the literature, while in Set B, epoxy is cured with a different weight percentage of phenalkamine (PA). For Set A, the critical mixture ratio adhered to established standards, maintaining a weight percentage of 100:10. In the case of Set B, various proportional compositions were explored, ranging from 100:10 to 100:100, as shown in Table 1. These compositions were mixed, poured into Mylar sheet-fold boxes, and allowed to cure for 24 h. Following this, a post-curing process was employed, subjecting all samples to a temperature of 80°C for 4 h. Notably, the composition ratio of 100:50 in Set B yielded optimal outcomes by achieving complete curing and resulting in a rigid polymer structure. We followed this optimum composition for further investigations.

Table 1: Composition of epoxy and PA in Set B

Types of composition (PA)	Epoxy (wt%)	PA (wt%)	Visual observation summary (24 h)
EP-10	100	10	No curing occurred
EP-20	100	20	Film cured, Less shrinkage
EP-30	100	30	Glossy surface, No shrinkage, Film layer formation internal uncured
EP-40	100	40	Glossy surface, Rigid sticky nature
EP-50	100	50	Glossy surface, Rigid structure
EP-60	100	60	Glossy surface, Rigid structure
EP-70	100	70	Glossy surface, Rigid structure
EP-80	100	80	Surface shrinkage, Moderate flexible
EP-90	100	90	Moderate flexible
EP-100	100	100	Surface shrink, High flexible

Further fiber reinforced laminated composites were prepared using a unidirectional glass fiber mat, which has areal density of 220 gsm. Two sets of composite laminates were prepared: one set of araldite epoxy resin (LY556) was cured with TETA based curative (HY951), and the other set was cured with PA in ratios of 100:10 and 100:50, respectively. GFRP composite laminates measuring 250×250 mm with specific fiber 12 layers of stacking zero degree orientation sequences were fabricated using compression molding. A non-adhesive insert (Teflon), approximately 13 microns thick, was placed in the neutral layer to act as a precrack layer within the mid-layer.

2.3 Characterization & Testing

The functional groups of EP-TETA and EP-PA polymer composite sheets were examined using FTIR spectroscopy (IRTRACER 100 Spectrophotometer, SHIMADZU, UK). The FTIR spectrum

range was maintained at 500 to 4000 cm^{-1} wave number. The morphology of the specimens was analysed by scanning electron microscopy (SEM), Vega3 Tescan, TESCAN, Czech Republic. For SEM, samples were taken from the tension test fractured region. The thermal degradation behaviour of bio-based cured epoxy composites was analysed using thermogravimetric analysis (TGA 4000, The Thermo Gravimetric Analyzer, PerkinElmer, Waltham, MA, USA). The differential scanning calorimetry (DSC) was used to explore the cure characteristics of the polymer composite by using the DSC instrument (The Setline DSC, SETARAM, Caluire-et-Cuire, Auvergne-Rhône-Alpes, France). A surface cure monitor (The GTC 600C InfraRed Camera, Bosch, Gerlingen, Baden-Württemberg, Germany) was used to observe the time and temperature effects on the surface curing process of both petroleum-based (TETA) and bio-based (PA) curatives in epoxy systems [25,26]. Additionally, the Arrhenius equation is applied to calculate the degree of cure, with the assistance of MATLAB code software [27,28].

Furthermore, the tensile strength, flexural strength, and single lap joint strength of both the pure epoxy matrix and bio-based epoxy composites were determined using a Tinus Olsen 100 kN instrument in accordance with ASTM-D638, ASTM-D790, and ASTM-D1002 standards, respectively. For fiber reinforced laminated composites, the above instrument was used to conduct end notch flexural (ENF) test following the ISO CD 15114 standard.

2.4 Determination of Epoxy Equivalent Weight (EEW)

For every 100 parts by weight of diglycidyl ether of bisphenol A (DGEBA), an epoxy resin, the recommended proportion of amine curative is calculated based on its molecular weight and the number of available hydrogens per mole. With the phenalkamine's molecular weight at 380.4 and four available hydrogens per mole, and considering the epoxy's equivalent weight at 190, the theoretical ratio for epoxy resin to amine curative is 1:0.5 parts, respectively.

3 Results and Discussion

3.1 FT-IR Spectrum of EP-PA

The functional groups associated with PA-cured epoxy polymers were observed by the FTIR analysis shown in Fig. 1. In the FTIR spectrumthe bands at 2920 and 2854 cm^{-1} are associated with both the C-H groups of the epoxy and the cardanol [8]. Peaks at 3003 cm^{-1} indicated C-H stretching characteristic of alkene, while the peak at 800 cm^{-1} implied C-H out-of-plane bending. The aromatic structure in cured sheet sample was confirmed by the peak at 1589 cm^{-1} representing C-C stretching. The peak at 1444 cm^{-1} assigned to the presence of a phenolic O-H bond. Additionally, the presence of a primary amine in PA was confirmed by the peak at 1028 cm^{-1}, corresponding to C-N stretching [29]. The peak at 1257 cm^{-1} is associated with the C-O-C stretching vibration of epoxy group. These findings provided valuable insights into the functional groups and structural characteristics of the PA-cured DGEBA epoxy resin sample [14].

3.2 Morphology Characteristics

Fig. 2a,b represents the surface morphology of the TETA & PA-cured epoxy systems. Fig. 2a depicts a rough surface with scale-like structures of EP-TETA possible due to the brittleness of the samples. On the other hand, the bio-based EP-PA system shows a smooth surface, indicating less brittleness. These SEM images suggested better compatibility with the PA-cured system (Fig. 2a). Brittle fractures are marked by a scale-like or rough texture with jagged, fragmented surfaces, signifying a sudden and catastrophic failure with minimal deformation. In contrast, non-uniform curing results in rough, uneven, or porous fracture surfaces with visible defects or voids, indicating an incomplete or inconsistent curing process. Ductile fractures display a smooth, wavy, or fibrous texture

with a plain surface, indicating a gradual failure accompanied by significant plastic deformation (Fig. 2b). Conversely, a uniform cure results in a smooth, even fracture surface with no porosity, voids, or defects, reflecting a consistent and complete curing process.
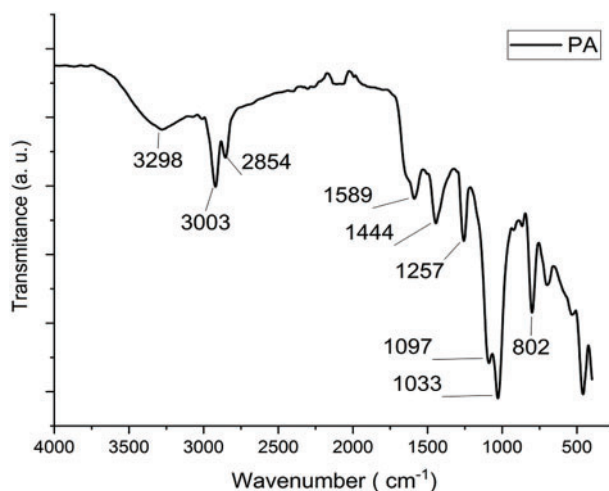

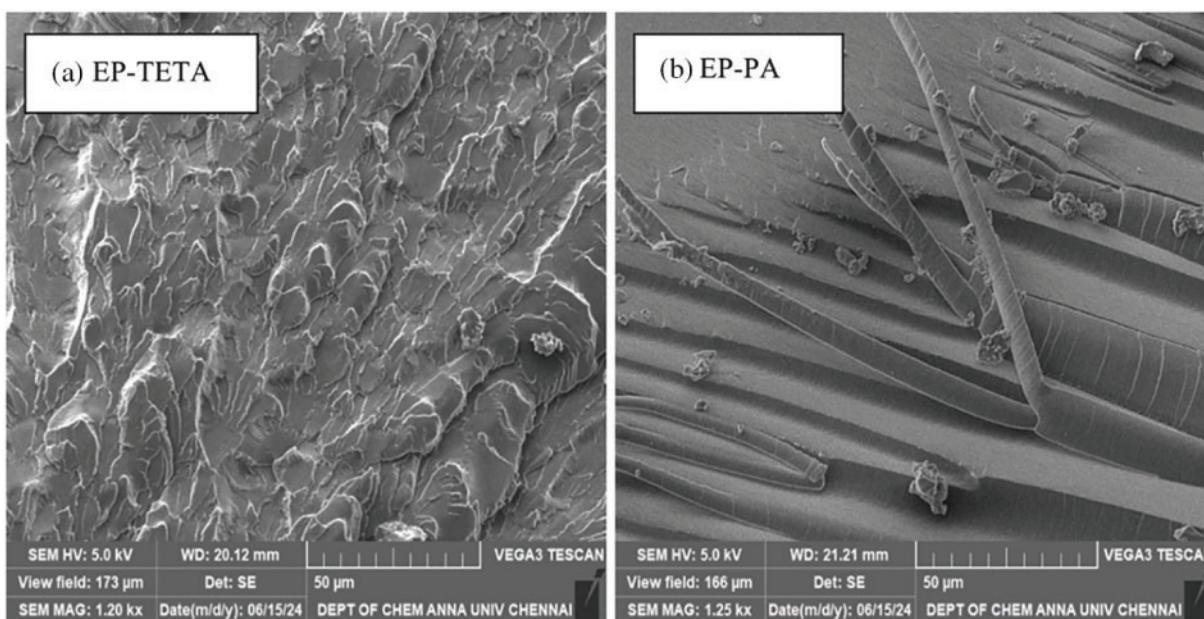**Figure 1:** FTIR analysis-PA cured specimen

Figure 2: SEM images of (a) TETA cured Epoxy (b) PA Cured

3.3 TGA Analysis of EP-PA

The thermal stability of EP-PA was determined by using TGA. Fig. 3 demonstrated that the onset of the degradation temperature was at 362°C and the maximum degradation temperature was at 430°C. Kathalewar et al. observed Epoxy-TETA-cured systems on-set degradation at 352°C and maximum degradation 488°C [10,19]. However, Fig. 3 reveals that the initial decomposition of the lengthy aliphatic chain present in the cardanol occurs at low temperatures, while the degradation of the crosslinked polymer is observed at elevated temperatures. During the initial stage of heating, the

epoxy-amine bonding was broken above 300°C and cleavage of the Mannich bridge occurred further up to 362°C. Beyond 430°C, it was observed that the compound decomposed into amines, phenolic substances, and benzene derivatives [21–23].
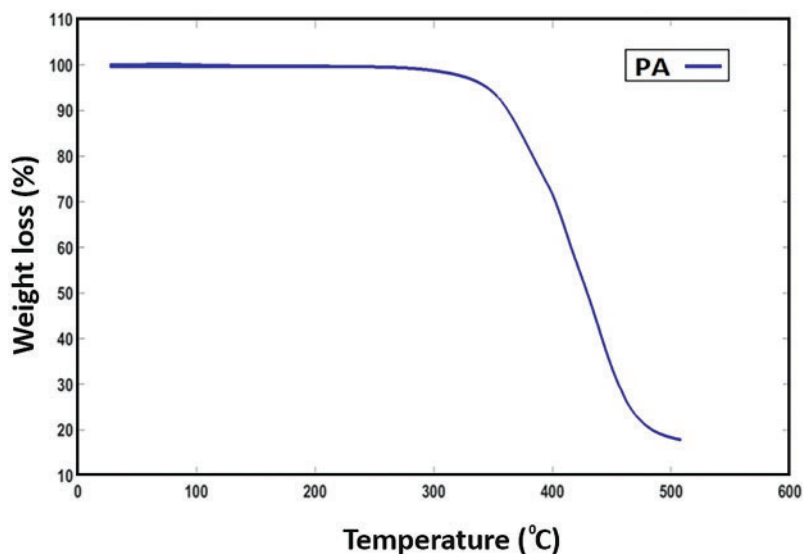

Figure 3: TGA analysis-PA cured specimen

3.4 Degree of Cure

We observed cure cross-linking kinetics via an IR camera, and exothermic reactions occurred during the low-temperature curing process of epoxy with PA-cured sheet samples (Fig. 4). Fig. 5a demonstrated that the time *vs*. temperature graph indicates low temperature cross-linking below 55°C temperature within 60 min. These results established the fast-crosslinking mechanisms and kinetics of the PA-cured epoxy system over the TETA-cured epoxy system by observing the initial temperature and fast conversion speed [29]. Additionally, the degree of cure was obtained from the collected data of surface temperature with time by using the Arrhenius Equation (Eq. (1)) with the help of MATLAB code. In the degree of cure *vs*. time plot (Fig. 5b), the phenalkamine-cured epoxy system exhibits an exothermic temperature rise up to 50°C. It shows lower surface energy and linear expansions compared to the TETA-cured epoxy system due to the presence of a side alkyl chain link, which may absorb the thermal energy. Here, the TETA-cured system displays high surface energy expulsion due to the exothermic reactions reaching up to 97°C [27,30].

Arrhenius Equation:

$$k = Ae^{\frac{-E_a}{RT}} \tag{1}$$

where, k is a degree of cure, A is pre-exponential factor, E_a isactivation energy (in the same units as R, T), R is Universal gas constant, T is Absolute temperature (in kelvin) [31,32].
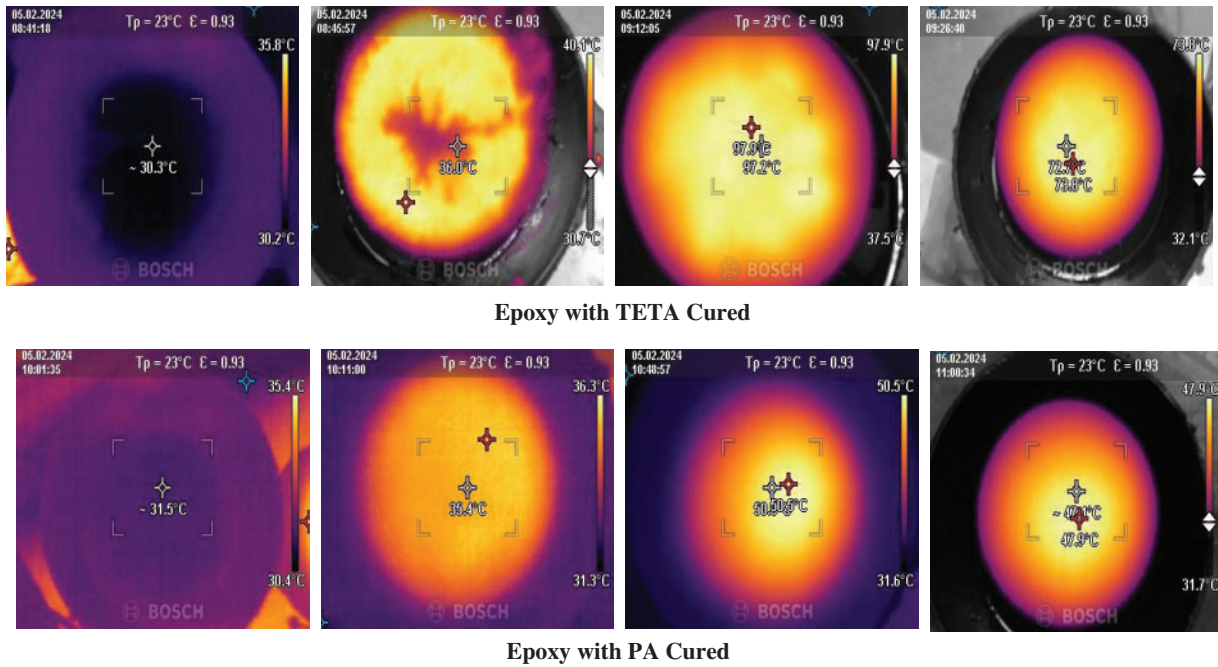
Epoxy with TETA Cured

Epoxy with PA Cured

Figure 4: IR thermograph images of surface temperature of epoxy with TETA and PA cured samples at variable time
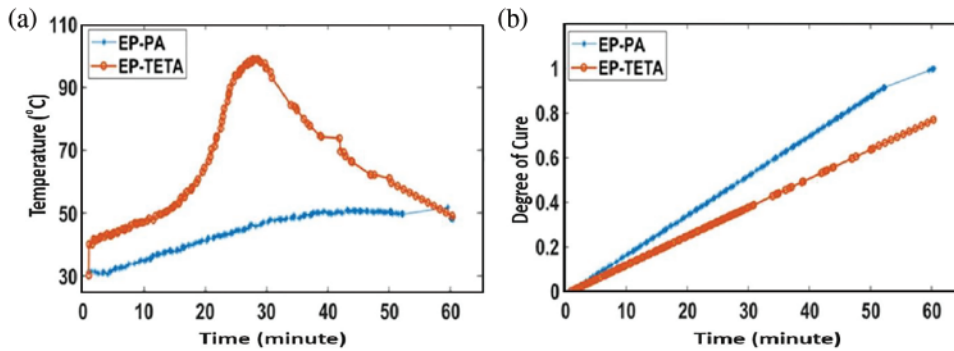

Figure 5: Degree of cure analysis using the Arrhenius Equation via MATLAB code. (a) Time *vs*. temperature graph using IR-thermograph setup, (b) Time *vs*. degree of cure graph

3.5 DSC Analysis of EP-PA

The cured compound behaviour of crosslinked epoxy sheet was examined by the DSC test method. Fig. 6 illustrates the glass transition temperature (Tg) at 101.4°C, which further confirms the crosslinking of epoxy with PA observed by IR real-time thermal imaging camera for surface cure kinetics [3]. This viscoelastic property of the polymer composite possibly occurs due to the presence of side chain long aliphatic group alignment controlling the viscosity and flexibility. Furthermore, Fig. 6 revealed complete curing of the samples beyond 101.4°C as there were no significant peaks for uncured residue. Therefore, it suggests that the curing process has effectively transformed the material into its fully-cured state without any remaining unreacted components. So, the flattened region of the curve from the temperature of 101.4°C to 250°C confirmed the complete cure of polymer composite samples.
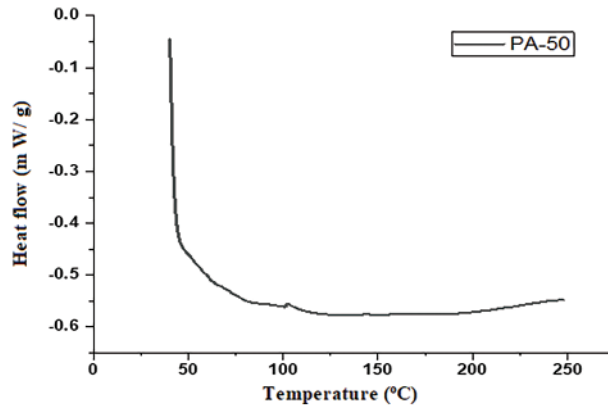
Figure 6: DSC analysis-PA cured specimen

3.6 Mechanical Testing

3.6.1 Tensile Test (ASTM D638-14) of EP-PA and EP-TETA

Epoxy resins are widely used in various industries due to their excellent mechanical properties, including their tensile strength and modulus. The tensile properties of EP-TETA and EP-PA were evaluated using Tinus Olsen 100 kN, and their results are shown in Table 2. The TETA-cured sample exhibited higher tensile force and tensile strength, signifying greater load-bearing capacity and strength. On the other hand, the PA sample demonstrated significantly greater elongation, indicating enhanced ductility and energy absorption. The tensile force, representing tensile strength, was higher in the TETA-Cured sample (839 N) than the PA sample (818 N). This indicates the former's greater resistance to deformation under tension. Tensile strength, accounting for applied force relative to the initial cross-sectional area, was also higher in the TETA Cured sample (19 MPa *vs*.15 MPa), emphasising its superior load-bearing capability. In this study, we observed comparable results with typical epoxy thermoset materials consisting of bio-based renewable toughening agents, which typically result in reduced stiffness and strength [33,34].

Table 2: Tensile characteristics of epoxy systems cured with TETA and PA

Sample	Tensile load (N)	Tensile strength (MPa)	Displacement (mm)
EP-TETA cured	839 ± 22	19 ± 0.83	3 ± 0.56
EP-PA cured	818 ± 15	15 ± 0.82	13 ± 0.95

The disparity in elongation before fracture, represented by the displacement, is quite pronounced between the EP-PA sample (13 mm) and the EP-TETA sample (3 mm). This distinction arises from varying crosslinking densities, which render cured epoxy either more rigid and resistant to plastic deformation during tensile elongation or more ductile and deformable. Consequently, EP-PA displays the highest elongation at break but the lowest tensile strength, whereas EP-TETA exhibits the opposite behaviour. This indicates that the EP-PA sample possesses greater ductility and deformability before reaching the breaking point, while the EP-TETA Cured sample experiences relatively less deformation before fracture. Furthermore, it's noteworthy that epoxy systems cured with phenalkamines having extended polyethylenepolyamine chains that tend to achieve a more balanced combination of mechanical and thermal properties [35,36]. TETA curing agents tend to produce stronger, more rigid materials, while PA agents yield more flexible and ductile ones. Therefore, material selection should align with

application requirements. The EP-TETA sample could be ideal for applications necessitating strength, while the EP-PA sample's greater deformability could be advantageous in scenarios requiring energy absorption and impact resistance.

3.6.2 Flexural Test (ASTM D790) of EP-PA and EP-TETA

The flexural properties of the EP-TETA and EP-PA were determined by using Tinus Olsen 100 kN. The flexural modulus is a measure of a material's stiffness in bending, as shown in Table 3. It quantifies how much a material will deform under a given bending stress. A higher flexural modulus indicates greater stiffness and resistance to deformation. In this work, EP-TETA exhibited a higher flexural modulus of 1.8 GPa, while EP-PA had a lower flexural modulus of 0.7 GPa. Fig. 7a suggests that the EP-TETA is stiffer and less prone to bending deformation compared to the EP-PA. Fig. 7b shows that the EP-PA sample deforms and does not break on applying maximum bending stress and is found to regain its original shape on removal of the load. This seems to be a special feature of EP-PA system. The higher ultimate stress and force exhibited by EP-PA suggest that it is more suitable for applications where bending strength is critical. On the other hand, EP-TETA's higher flexural modulus indicates that it may be better suited for applications requiring structural rigidity and minimal deformation under bending loads.

Table 3: Flexural performance of EP-TETA and EP-PA

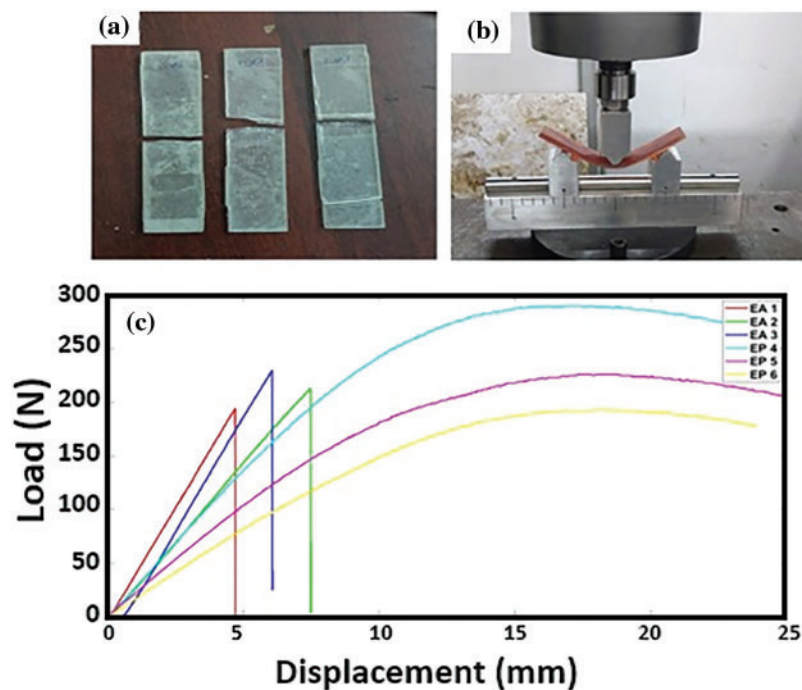| Sample	Flexural load (N)	Flexural stress (MPa)	Flexural modulus (GPa)
EP-TETA cured	212 ± 14	34 ± 0.5	1.8 ± 0.18
EP-PA cured	236 ± 12	49 ± 0.19	0.7 ± 0.09

Figure 7: Flexural samples (a) Epoxy with TETA fractured specimen (b) Epoxy with PA during flexural test (c) Load *vs*. Displacement curve

The differences in mechanical properties can be attributed to the type of curing agent used for each sample. Different curing agents can result in varying degrees of cross-linking and material behaviour. Fig. 7c revealed that EP-TETA's higher stiffness might be due to a higher degree of crosslinking, while the PA sample's increased flexibility and strength might be attributed to a different curing mechanism [7]. Therefore, the flexural test results highlight the differences in bending properties between EP-TETA and EP-PA. The EP-PA demonstrated higher ultimate stress, force, and flexibility, making it more suitable for applications requiring bending strength and ductility [34]. On the other hand, EP_TETA's higher flexural modulus suggests it's better suited for applications demanding structural rigidity and minimal deformation. The choice between these materials depends on the specific mechanical requirements of the intended application.

3.6.3 Impact Test (ASTM D6110) of EP-PA and EP-TETA

The impact resistance of the EP-TETA and EP-PA was determined using an impact tester. Table 4 represents the substantial difference in impact resistance between EP-TETA and EP-PA. It suggests that the PA material has a greater ability to absorb energy from sudden impacts, making it more suitable for applications where impact resistance is a crucial factor. This could be advantageous in scenarios where the material is subjected to dynamic loading or potential impacts, such as in protective equipment, automotive components, or structures prone to impact forces. The differences in impact resistance can be attributed to the material's inherent properties, including its molecular structure, toughness, and ability to deform and absorb energy without fracturing. EP-PA often results in more ductile and tough materials, leading to improved impact resistance. In contrast, TETA-cured materials might exhibit a higher level of brittleness, resulting in lower impact resistance.

Table 4: Toughness of TETA cured & PA cured epoxy system

Sample	Impact resistance (J/m)
EP-TETA cured	27.3 ± 2.2
EP-PA cured	115.9 ± 3.4

The impact test results provide valuable insights into material selection for various applications. If impact resistance is a critical requirement, the PA material appears to be a better choice due to its higher energy absorption capacity. However, it's important to note that other factors, such as mechanical properties, chemical compatibility, and cost, should also be considered when selecting a material for a specific application.

3.6.4 Single Lap Joint Test (ASTM D1002)

The bonding strength of the EP-TETA and EP-PA was evaluated by a single-lap joint test. From Fig. 8a, it was observed that the distinct failure modes have occurred in two different curing systems. The EP-TETA system exhibits adhesion failure, where the separation occurs primarily at the interface between two materials, indicating a weaker bond between them. Cracks developed at the extremities of the overlap within the adhesive material and extended inward towards the interface between the adhesive and the adhered [37].

The propagation direction of these cracks was primarily influenced by the maximum principal stress within the adhesive. On the other hand, shown in Fig. 8b, EP-PA shows a cohesive failure region, implying that the failure primarily occurs within the material itself, suggesting stronger internal cohesion and bonding within the system [38]. A coarse adhesive surface can be observed, indicating the occurrence of a cohesive failure mode, as shown in Fig. 8c. The EP-PA adhesive exhibited higher

ultimate force and stress. Table 5 highlights its stronger bonding capabilities. Both adhesives had similar breaking distances, but the EP-PA adhesive is preferable for applications requiring robust adhesion. The higher ultimate force and stress exhibited by the EP-PA adhesive suggest that it offers stronger bonding capabilities compared to the EP-TETA adhesive. This makes the EP-PA adhesive a preferable choice for applications requiring robust adhesion and load-bearing capacity [21].
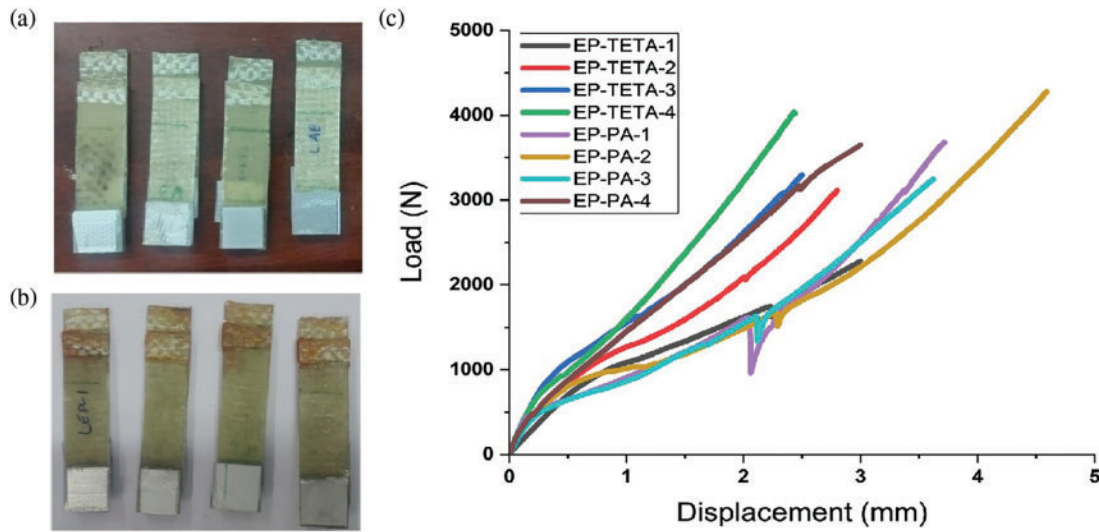

Figure 8: SLJ test samples (a) Fractured samples (LAE-Lap Joint TETA cured) (b) LEP-(Joint PA cured) (c) Load-displacement curve

Table 5: Effects of SLJ on EP-TETA and EP-PA

Cured sample	Ultimate force (N)	Ultimate stress (MPa)	Displacement (mm)
EP-TETA	3620 ± 14	85 ± 0.45	3.40 ± 0.2
EP-PA	$4220 + 18$	$99 + 0.56$	$3.62 + 0.3$

The differences in adhesive performance can be attributed to various factors, including the type of adhesive, curing mechanisms, and molecular interactions between the adhesive and the substrates being joined. The specific curing characteristics of the EP-PA adhesive might result in stronger bonds and higher adhesion performance. The process of crosslinking the polymer chains enhances both the flexibility and the elastic threshold of the EP-PA [39,40]. The single-lap joint test results have implications for material selection in applications requiring bonded components. The higher ultimate force and stress exhibited by the EP-PA adhesive make it suitable for applications where reliable adhesion and strength are vital, such as in structural assemblies or load-bearing joints.

3.6.5 Flexural Testing in Mode II for Interlaminar Properties

The interlaminar properties of EP-PA and EP-TETA fiber reinforced laminated sheets were tested by a three-point bending test in Tinus Olsen100 kN (Mode II). The test was initiated after a 40 mm crack was first observed in the specimen. In the end-notch flexural (ENF) test, failure is attributed to interlaminar shear occurring within the midplane of the laminate. This failure mode is induced by the presence of a pre-existing teflon crack, leading to crack propagation parallel to the fiber direction. The Mode II fracture toughness value, GIIC, was calculated using the following equations (Eqs. (2) and (3)):

$$G_{IIC} = \frac{9P\delta a^2}{2B\left(\frac{1}{4L^3} + 3a^3\right)} \tag{2}$$

where, a is delamination crack length (mm), δ is displacement (mm), P is maximum load (N), B is width of specimen (mm) [22].

$$E = \frac{L^3 P}{Abh^3\delta} \tag{3}$$

In Eq. (3), E represents the flexural modulus, typically measured in units of MPa or GPa. L denotes the span length of the specimen, measured in millimetres (mm). And δ signifies the displacement caused by load F during flexure, measured from the initial position. P indicates the applied load, measured in Newtons (N). The variables b and h represent the width and height of the specimen, respectively, also measured in millimeters (mm) [22].

Fig. 9a depicts the load-displacement curve of glass Fiber with PA curing (GEP-PA). In the initial region, the graph exhibits a linear rise. After a certain point, there is a load disruption, followed by another increase. This behavior might be attributed to the matrix's capability to endure higher toughness by hindering crack advancement. In contrast, glass Fiber with TETA cure (GEP-TETA) has an initial linear appearance in the first region, corresponding to the composite laminate's elastic deformation. In the subsequent region, a peak load rise is observed, followed by a decline due to load failure.
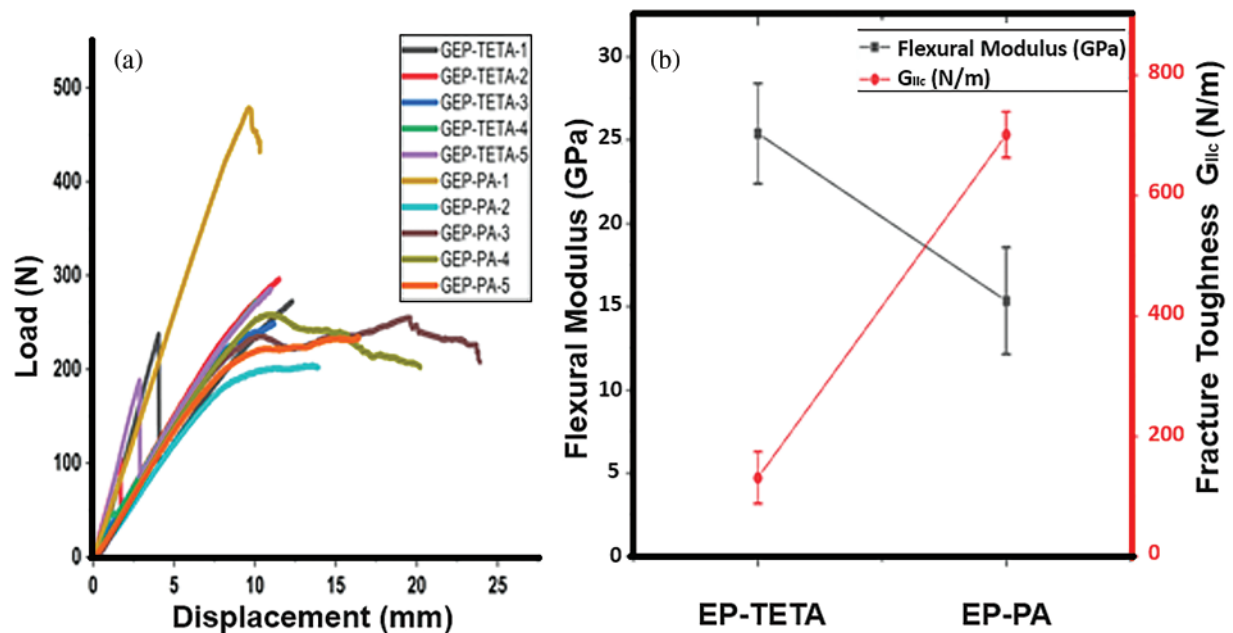

Figure 9: Flexural testing in Mode II for interlaminar properties (a) Load *vs*. displacement curve (b) Interlaminar fracture toughness of GEP-EP & GEP-TETA samples, respectively

A noticeable contrast: the interlaminar fracture toughness of GEP-PA surpasses that of GEP-TETA (Fig. 9b). This observation signifies a more robust bonding between the fiber and matrix, consequently leading to enhanced interlaminar fracture toughness. Additionally, this heightened adhesion resists the initiation of microcracks by facilitating supplementary energy dissipation mechanisms, such as debonding [8]. Fig. 9 also illustrates a 5.3 timesrise in the interlaminar fracture toughness of

GEP-PA compared to GEP-TETA [39,40]. This discrepancy might stem from the inherent brittleness of epoxy when coupled with TETA, leading to a reduction in interlaminar fracture toughness [40].

4 Conclusion

In this study, epoxy was cured using synthetic (TETA) and biobased curing agents (PA), and composite sheets were prepared and characterized. The results of various mechanical tests, including tensile, flexural, impact, SLJ tests, and ENF tests, were conducted and observed to determine the material's behaviour and suitability for different possible applications. EP-TETA exhibited approximately a 2.6% higher tensile strength compared to EP-PA, suggesting its improved resistance to deformation under tension and making it a preferable choice for applications requiring high strength. Additionally, EP-TETA exhibited approximately 28% higher tensile strength compared to EP-PA, further emphasising its superior load-bearing capability. But EP-PA displayed a breaking distance approximately 318% greater than that of EP-TETA, indicating its substantial improvement in ductility and deformability. Also, PA excels in ultimate stress and force, making it a suitable choice for applications prioritising bending strength and ductility. The single-lap joint test revealed distinct failure modes. EP-TETA material exhibited adhesion failure, while EP-PA material showed cohesive failure, indicating stronger internal cohesion. EP-PA exhibited approximately 16% higher force and strength, making it a superior choice for applications demanding robust adhesion and load-bearing capacity. Additionally, superior interlaminar fracture toughness enhanced adhesion resisted microcrack initiation, and led to a 5.3 times higher interlaminar fracture toughness for GEP-PA compared to GEP-TETA. The EP-PA thermosets exhibited commendable mechanical and thermal properties, underscoring their significant potential for use as top-tier, bio-based epoxy thermosetting materials. These materials hold promise for applications in coatings, the automobile, the aerospace industry, and electronic components, offering a sustainable alternative that can partially replace petroleum-based thermosetting materials loading into the bio-based volume of 0.7:0.3 in unit volume to form the sustainable-based eco-system.

Author Contributions: Aswinraj Anbazhagan: Conceptualization, Methodology, Formal Analysis, Writing—Original Draft, Visualization; Sahila Sambandam: Data Curation; Piyali Roy Choudhury: Writing—Review & Editing, Investigation; Jayakumari Lakshmanan Saraswathi: Investigation, Supervision. All authors reviewed the results and approved the final version of the manuscript.

Availability of Data and Materials: The authors confirm that the data supporting the findings of this study are available within the article its supplementary materials.

Ethics Approval: Not applicable.

Conflicts of Interest: The authors declare no conflicts of interest to report regarding the present study.

References

1. Agarwal G. Comparative investigations on fracture toughness and damping response of fabric reinforced epoxy composites. J Polym Mater. 2023 May;39(3–4):255–67. doi:10.32381/JPM.2022.39.3-4.6.

2. Bhatt D, Patel RP, Parsania JHP. Fabrication and comparative properties of sustainable epoxy Methacrylate of Bisphenol-C-Jute/treated jute-natural fibers sandwich composites: part-2. J Polym Mater. 2023;39(3–4):223–39. doi:10.32381/JPM.2022.39.3-4.4.

3. Chopda DB, Saurashtra JV, Parsania PH. Curing kinetics of epoxy resin of (2E, 6E) 2,6-bis (4-hydroxy benzylidene) cyclohexanone. J Polym Mater. 2022;38(1–2): 11–9. doi:10.32381/JPM.2021.38.1-2.2.

4. Huang K, Zhang Y, Li M, Lian J, Yang X, Xia J. Preparation of a light color cardanol-based curing agent and epoxy resin composite: cure-induced phase separation and its effect on properties. Prog Org Coat. 2012;74(1):240–7. doi:10.1016/j.porgcoat.2011.12.015.

5. Devi V, Selvaraj M, Selvam P, Kumar AA, Sankar S, Dinakaran K. Preparation and characterization of CNSR functionalized Fe_3O_4 magnetic nanoparticles: an efficient adsorbent for the removal of cadmium ion from water. J Environ Chem Eng. 2017;5(5):4539–46. doi:10.1016/j.jece.2017.08.036.

6. Nabipour H, Rohani S, Hu Y. A bio-based vanillin ligand to remove silver ions from a waste stream and utilizing it to improve the fire safety of an epoxy thermoset and its thermal conductivity. J Environ Chem Eng. 2024;12:112121. doi:10.1016/j.jece.2024.112121.

7. Zhang J, Xu S. Effect of chain length of cardanol-based phenalkamines on mechanical properties of air-dried and heat-cured epoxies. Mater Express. 2019;9:337–43. doi:10.1166/mex.2019.1498.

8. Tzatzadakis V, Tserpes K. Experimental characterization of the hygrothermal ageing effects on the bulk mechanical properties and lap-shear strength of the novel bio-based epichlorohydrin/cardanol adhesive. J Adhes. 2022;98:49–67. doi:10.1080/00218464.2020.1817742.

9. Venkatesan DB, Vellayaraj A. The effect of adhesively bonded external hybrid patches on the residual strength of repaired glass/epoxy-curved laminates. Polym Compos. 2024;45:3493–506. doi:10.1002/pc.28004.

10. Kathalewar M, Sabnis A. Effect of molecular weight of phenalkamines on the curing, mechanical, thermal and anticorrosive properties of epoxy based coatings. Prog Org Coat. 2015;84:79–88. doi:10.1016/j.porgcoat.2015.02.014.

11. Ikeda R, Tanaka H, Uyama H, Kobayashi S. Synthesis and curing behaviors of a crosslinkable polymer from cashew nut shell liquid. Polymer. 2002;43:3475–81. doi:10.1016/S0032-3861(02)00062-9.

12. Lal SS, Kannan S, Sahoo SK. Influence of flax fiber orientation on mechanical, thermo-mechanical and interfacial adhesion properties of epoxidized methyl ricinoleate modified epoxy composite: a sustainable green composite for cleaner production. Mater Today Commun. 2022;33:104648. doi:10.1016/j.mtcomm.2022.104648.

13. Manjare SB, Chaudhari RA. Environment-friendly synthesis of palladium nanoparticles loaded on Zeolite Type-Y (Na-form) using Anacardium Occidentale shell extract (Cashew nut shell extract), characterization and application in –C–C– coupling reaction. J Environ Chem Eng. 2020;8:104213. doi:10.1016/j.jece.2020.104213.

14. Kaur M, Jayakumari LS. Eco-friendly cardanol-based phenalkamine cured epoxy-cenosphere syntactic foams: fabrication and characterisation. J Appl Polym Sci. 2016;133:147. doi:10.1002/app.44189.

15. Bo C, Shi Z, Hu L, Pan Z, Hu Y, Yang X, et al. Si and N based precursors to develop flame retardant phenolic foam. Sci Rep. 2020;10:12082. doi:10.1038/s41598-020-68910-6.

16. Farias da Silva JMF, Soares BG. Epoxidized cardanol-based prepolymer as promising biobased compatibilizing agent for PLA/PBAT blends. Polym Test. 2021;93:106889. doi:10.1016/j.polymertesting.2020.106889.

17. Venkatesan DB, Vellayaraj A, Chelliah SK. The influence of thickness and recycled milled glass fiber fillers on the delamination resistance of polymer composite angle brackets. Polym Compos. 2024;45:3067–80. doi:10.1002/pc.27971.

18. Mi X, Liang N, Xu H, Wu J, Jiang Y, Nie B, et al. Toughness and its mechanisms in epoxy resins. Prog Mater Sci. 2022;130:100977. doi:10.1016/j.pmatsci.2022.100977.

19. Elango I, Santulli C, Vellayaraj A. A novel approach to enhance the mechanical behavior of glass epoxy laminates with sustainable recycled milled fillers. Polym Compos. 2024;45:5416–29. doi:10.1002/pc.28136.

20. Da Silva LFM, Rodrigues TNSS, Figueiredo MAV, De Moura MFSF, Chousal JAG. Effect of adhesive type and thickness on the lap shear strength. J Adhes. 2006;82:1091–115. doi:10.1080/00218460600948511.

21. Tserpes K, Tzatzadakis V. Life-cycle analysis and evaluation of mechanical properties of a bio-based structural adhesive. Aerospace. 2022;9:64. doi:10.3390/aerospace9020064.

22. De Baere I, Jacques S, Van Paepegem W, Degrieck J. Study of the Mode I and Mode II interlaminar behaviour of a carbon fabric reinforced thermoplastic. Polym Test. 2012;31:322–32. doi:10.1016/j.polymertesting.2011.12.009.

23. Sajith S, Arumugam V, Dhakal HN. Effects of curing pressure on mode II fracture toughness of unidirectional GFRP laminates. Polym Test. 2015;48:59–68. doi:10.1016/j.polymertesting.2015.09.011.

24. Zulkifl R, Azhari CH. Mode II interlaminar fracture properties of treated silk fibre/epoxy composites at low and high temperature range. Int J Eng Technol. 2018;7:129. doi:10.14419/ijet.v7i3.17.16636.

25. Gliszczynski A, Wiącek N. Experimental and numerical benchmark study of mode II interlaminar fracture toughness of unidirectional GFRP laminates under shear loading using the end-notched flexure (ENF) test. Compos Struct. 2021;258:113190. doi:10.1016/j.compstruct.2020.113190.

26. Kateb B, Yamamoto V, Yu C, Grundfest W, Gruen JP. Infrared thermal imaging: a review of the literature and case report. NeuroImage. 2009;47:T154–62. doi:10.1016/j.neuroimage.2009.03.043.

27. Knobloch M, Lottermoser BG. Infrared thermography: a method to visualise and analyse sulphide oxidation. Minerals. 2020;10:933. doi:10.3390/min10110933.

28. Hardis R, Jessop JLP, Peters FE, Kessler MR. Cure kinetics characterization and monitoring of an epoxy resin using DSC, Raman spectroscopy, and DEA. Compos Part Appl Sci Manuf. 2013;49:100–8. doi:10.1016/j.compositesa.2013.01.021.

29. Crapse J, Pappireddi N, Gupta M, Shvartsman SY, Wieschaus E, Wühr M. Evaluating the Arrhenius equation for developmental processes. Mol Syst Biol. 2021;17:e9895. doi:10.15252/msb.20209895.

30. Ran Q, Gu Y, Ishida H. Thermal degradation mechanism of polybenzoxazines. In: Advanced and emerging polybenzoxazine science and technology. Amsterdam: Elsevier; 2017. p. 171–204. doi:10.1016/B978-0-12-804170-3.00011-1.

31. Wazarkar K, Sabnis AS. Phenalkamine curing agents for epoxy resin: characterization and structure property relationship. Pigment Resin Technol. 2018;47:281–9. doi:10.1108/PRT-08-2017-0071.

32. Roşu D, Caşcaval CN, Mustątă F, Ciobanu C. Cure kinetics of epoxy resins studied by non-isothermal DSC data. Thermochim Acta. 2002;383:119–27. doi:10.1016/S0040-6031(01)00672-4.

33. Samyn P, Bosmans J, Cosemans P. Benchmark study of epoxy coatings with selection of bio-based phenalkamine versus fossil-based amine crosslinkers. Molecules. 2023;28:4259. doi:10.3390/molecules 28114259.

34. Bernath A, Kärger L, Henning F. Accurate cure modeling for isothermal processing of fast curing epoxy resins. Polymers. 2016;8:390. doi:10.3390/polym8110390.

35. Mi X, Wei F, Zhong L, Zeng L, Zhang J, Xu Z, et al. Epoxidation of agricultural byproduct konjac fly powder and utilization in toughening and strengthening epoxy resin. Ind Crops Prod. 2020;146:112161. doi:10.1016/j.indcrop.2020.112161.

36. Naik N, Shivamurthy B, Thimmappa BHS, Guo Z, Bhat R. Bio-based epoxies: mechanical characterization and their applicability in the development of eco-friendly composites. J Compos Sci. 2022;6:294. doi:10.3390/jcs6100294.

37. Devi A, Srivastava D. Studies on the blends of cardanol-based epoxidized novolac type phenolic resin and carboxyl-terminated polybutadiene (CTPB), I. Mater Sci Eng A. 2007;458:336–47. doi:10.1016/j.msea.2006.12.081.

38. Panda R, Tjong J, Nayak SK, Sain MM. Effect of Alkyl Phenol from cashew nutshell liquid on mechanical and dry sliding wear behavior of epoxy resin. BioResources. 2015;10:4126–36. doi:10.15376/biores.10.3.4126-4136.

39. Ortega-Iguña M, Chludzinski M, Sánchez-Amaya JM. Comparative mechanical study of pressure sensitive adhesives over aluminium substrates for industrial applications. Polymers. 2022;14:4783. doi:10.3390/polym14214783.

40. Shang X, Marques EAS, Carbas RJC, Barbosa AQ, Jiang D, Da Silva LFM, et al. Fracture mechanism of adhesive single-lap joints with composite adherends under quasi-static tension. Compos Struct. 2020;251:112639. doi:10.1016/j.compstruct.2020.112639.